Pezeshki and Ahmadi *Journal of Theoretical and Applied Physics* 2012, **6**:12
http://www.jtaphys.com/content/6/1/12

Journal of Theoretical and Applied Physics
a SpringerOpen Journal

RESEARCH Open Access

Nanoscale effects on multichannel add/drop filter based on 2-D photonic crystal ring-resonator heterostructure

Hamed Pezeshki[1] and Vahid Ahmadi[2*]

Abstract: In this paper, we propose a heterostructure multichannel add/drop filter based on 2-D photonic crystal ring-resonator in which, add and drop operations are accomplished by coupling between two W1 waveguides. The wavelength spacing of 10.3 nm, as well as the average cross-talk of −37.5 dB, are the other features of the proposed filter. Furthermore, nanoscale effects on the filter's performance including wavelength spacing, cross-talk amount, and dynamic response are considered. By taking into account these effects, the minimum wavelength spacing of 12 nm is obtained, whereas the filter's cross-talk has an average of −40 dB. Simulations are performed using 2-D finite-difference time-domain calculations.

Keywords: Photonic crystal, Multichannel add/drop filter, Ring-resonator, Heterostructure, Nanoscale effect

PACS: 42.70.Qs, 42.79.Ci, 42.79.Sz, 42.82.Et

Background

Photonic crystals (PHCs) with periodic dielectric materials have provided new ways of controlling light by means of photonic band gap (PBG). The PBG is a frequency gap in which the propagation of incident light with special frequencies as well as special polarization will be possible. This feature, in turn, has been utilized for realization of new optical functionalities and many novel devices. During the last decade, photonic crystals have been the most important part in the different areas of engineering consisting of coherent electron-photon interactions, ultra small add/drop filters (ADFs), low threshold lasers, photonic chips, nonlinear optics, and quantum information processing [1-7]. PHCs with photonic band gap guidance mechanism can provide highly confined guided mode which is suitable for controlling the propagation of light [8]. Nowadays, all-optical ADFs are the basis of wavelength division multiplexer telecommunication systems. On the other hand, compactness is an important issue for future all-optical integrated circuits. Hence, one of the most important candidates for constructing ultra small ADFs without significant losses are photonic crystal ring-resonators (PCRRs), where the guided mode is coupled between two W1 waveguides. Two specific properties of such devices are high quality factor (Q-factor) and small modal volume (V). Having a high Q-factor gives rise to the selectivity of filters, and small V provides single-mode operation. High Q-factor plus small V, together with PBG guidance mechanism, lead to improve the performance of small ADF based on PCRRs compared to conventional micro-ring-resonators-based bulk dielectric.

In this paper, a multichannel ADF based on 2-D PCRR is proposed in which the wavelength spacing of 10.3 nm and average cross-talk of −37.5 dB are obtained. Furthermore, nanoscale effects on the ADF's performance for the first time, to the best of our knowledge, are investigated. The minimum wavelength spacing of 12 nm and average cross-talk of −40 dB are the results of ADF with the structure of nanoscale rods. The filter's dynamic response is determined by using fast picoseconds Gaussian pulses, and the 2-D finite-difference time-domain (FDTD) method is applied.

* Correspondence: v_ahmadi@modares.ac.ir
[2]Department of Electrical and Computer Engineering, Tarbiat Modares University, Tehran 14115-194, Iran
Full list of author information is available at the end of the article

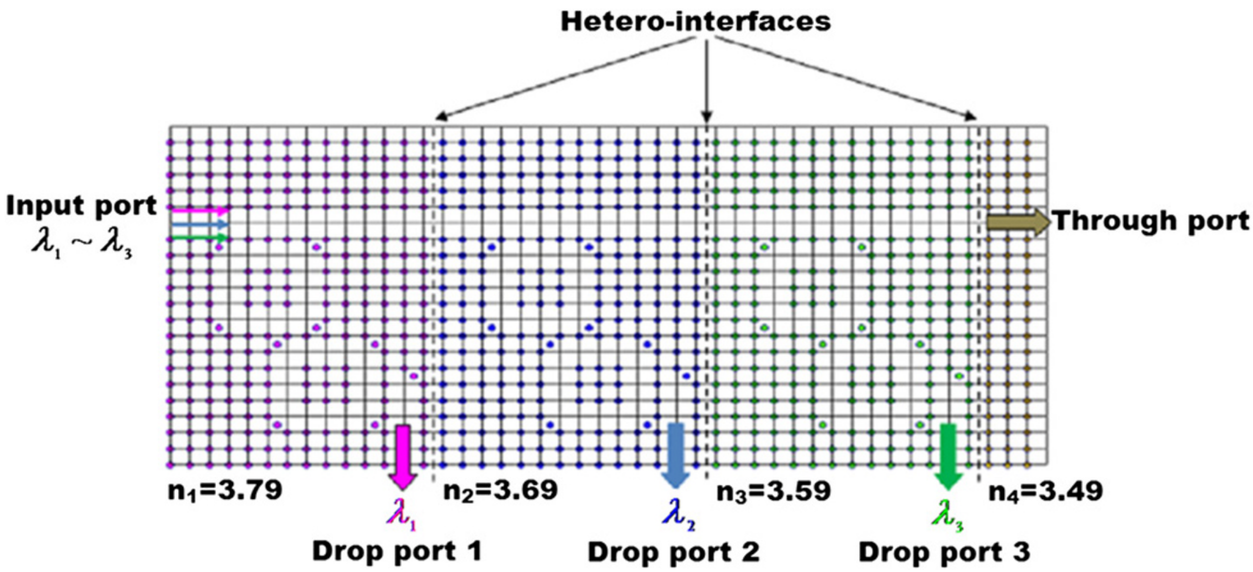

Figure 1 Schematic structure of multichannel ADF based on 2-D PCRR hetero-structure.

Results and discussion

Structure design

The multichannel ADF structure is composed of 2-D PCRR where PHC has a square dielectric-rod lattice. The lattice constant (a) and the radius of rods (r) are 540 nm and 0.185a (≈100 nm), respectively. The schematic structure is sketched in Figure 1. As shown in this figure, the filter is composed of four parts with different refractive indices where three parts of them look similar in their structure. Moreover, those rods at the corner of each ring are used to reduce the radiation losses of light mode's energy from the ring corners [9]. They have the same radius and refractive index like the other rods in that corresponding part. Furthermore, the last part at

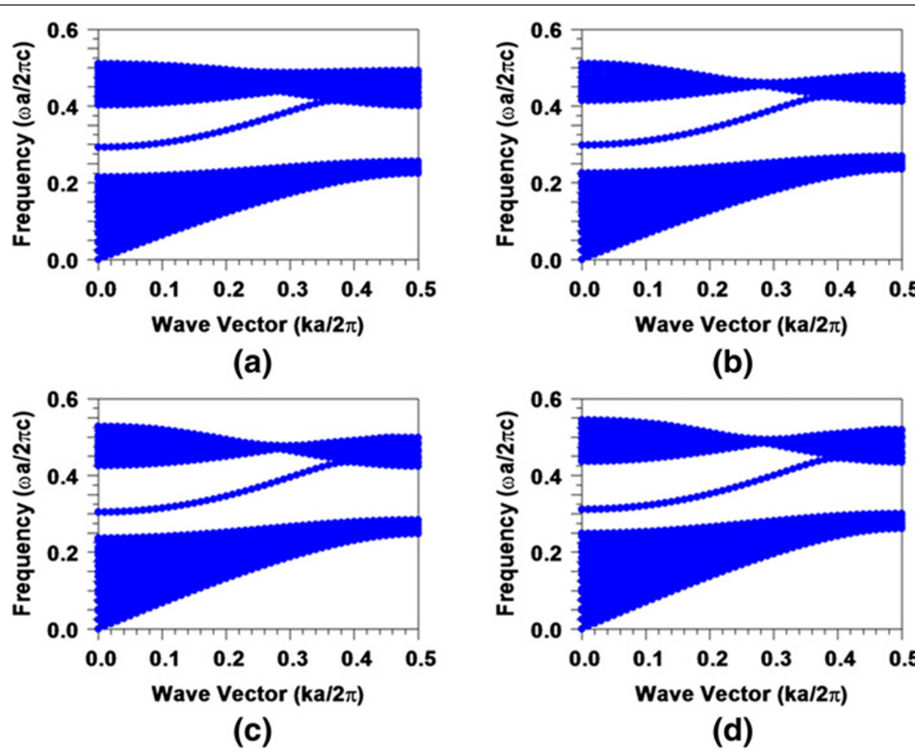

Figure 2 Dispersion curves of W1 waveguide for different refractive indices of: a) 3.79, b) 3.69, c) 3.59, and d) 3.49.

the right side is assigned to improve the efficiency of channel 3. Both ring-resonators in each part are similar. Since the coupling mechanism in this kind of structure is utilized between waveguides, we have to take advantage of its heterostructure technology. This technique is employed by considering the fact that each adjacent part has a different index of refraction. Indices of parts are chosen from left to right 3.79, 3.69, 3.59, and 3.49, respectively. As mentioned in [10], the band diagram of each PHC will be scaled with the change of lattice constant as well as refractive index. That is, the same band diagram can be achieved, but with this difference, the operational wavelength varies in conjunction with changes in refractive index or lattice constant of the structure. The dispersion curves for each part of the structure are illustrated in Figure 2, and the operational frequency range of guided mode for all parts is listed in Table 1. As shown in Figure 2, a change in the refractive index of waveguide's rods causes a change in the dispersion curve. Changes in frequency range of guided mode are inversely proportional with the change in refractive index. According to Table 1 in this structure, the common frequency is almost in the range of 0.3182 to 0.43035 ($\omega a/2\pi c$), where ω and c are frequency and speed of light in vacuum, respectively.

Add and drop operation

Output properties of this filter are analyzed using 2-D FDTD method by injecting the pulse train including three Gaussian pulses with full-width-at-half-maximum (FWHM) of 6 ps by the same input power but at different wavelengths. First, we find the resonant wavelength

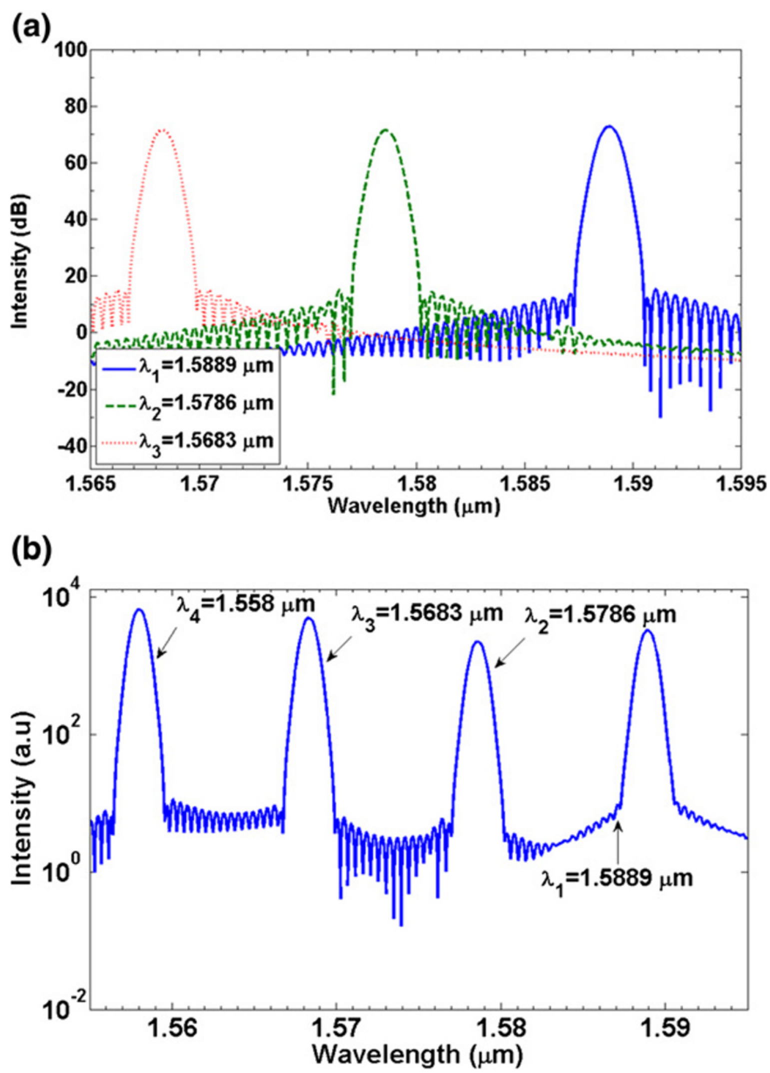

Figure 3 Add/drop spectra of proposed multichannel ADF. (a) Drop spectra of proposed multichannel ADF based on 2-D PCRR for Guassian input pulse with FWHM of 6 ps (**b**) Add spectra of proposed multichannel ADF based on 2-D PCRR. The signal λ_4 is injected from input port.

Table 1 Frequency range of W1 waveguide's guided single mode for different refractive indices

Refractive index	Frequency range ($\omega a/2\pi c$)	Corresponding dispersion curve
$n_1 = 3.79$	0.2981 ~ 0.4304	Figure 2a
$n_2 = 3.69$	0.3042 ~ 0.4399	Figure 2b
$n_3 = 3.59$	0.3109 ~ 0.4484	Figure 2c
$n_4 = 3.49$	0.3182 ~ 0.4578	Figure 2d

for the part of structure with refractive index of 3.59 is 1.5683 μm by sweeping the wavelength parameter of input Gaussian pulse around the wavelengths of 1.5-1.6 μm. From Figure 2c, the corresponding wave vector is obtained. Then according to the wave vector and Figure 2a,b, the corresponding wavelengths of the other parts with refractive indices of 3.69 and 3.79 are obtained as 1.5786 μm and 1.5889 μm, respectively. Figures 3 and 4 illustrate add/drop spectra of the proposed filter, and light propagation inside the multichannel filter simulated by 2-D FDTD for wavelengths of $\lambda_1 = 1.5589$ μm, $\lambda_2 = 1.5786$ μm, and $\lambda_3 = 1.5683$ μm, respectively. Considering the results shown in Figure 3, we obtained the parameters such as output FWHM, *Q*-factor, cross-talk, and time response which are specified in Table 2. According to Table 2, the difference between the channel's outputs FWHM is 0.02 nm. Moreover, the *Q*-factors are nearly the same and for wavelength spacing of 10.3 nm, the average cross-talk of filter has been −37.5 dB. Also, the time response (i.e., dynamic response) of each channel to the input excitation is determined and listed in Table 2. The average time response of filter and the difference between time responses of output channels are 4.78 and 0.14 ps, respectively.

To demonstrate the add operation, Gaussian pulses with wavelengths of $\lambda_1 = 1.5589$ μm, $\lambda_2 = 1.5786$ μm, and $\lambda_3 = 1.5683$ μm are injected from the corresponding drop ports simultaneously together with $\lambda_4 = 1.558$ μm from input port. Figure 3b represents add spectra of proposed filter which is monitored from through port. Moreover, the add operations for λ_1~λ_3 are performed correctly. In addition, we select the wavelengths based on Metro Coarse Wavelength Division Multiplexing Wavelength Grid as specified by International Telecommunication Union-Telecommunication Standardization Sector G.649.2 [11] from L band. Our proposed filter which is based on double ring-resonators 2-D PHC heterostructure has better performances like wavelength spacing and output bandwidth compared to the structures in [8,12-15]. The ADFs reported in [8,15] are based on 2-D PCRR in which the wavelength spacing in each case are 240 nm and above 20 nm, respectively. In addition, the ADFs presented in [12-14] are based on 2-D PHC cavity with the average wavelength spacing of more than 20 nm. Consequently, one can deduce that the output channels in our proposed structure have narrower bandwidths as well as much smaller wavelength spacing. These two fundamental features

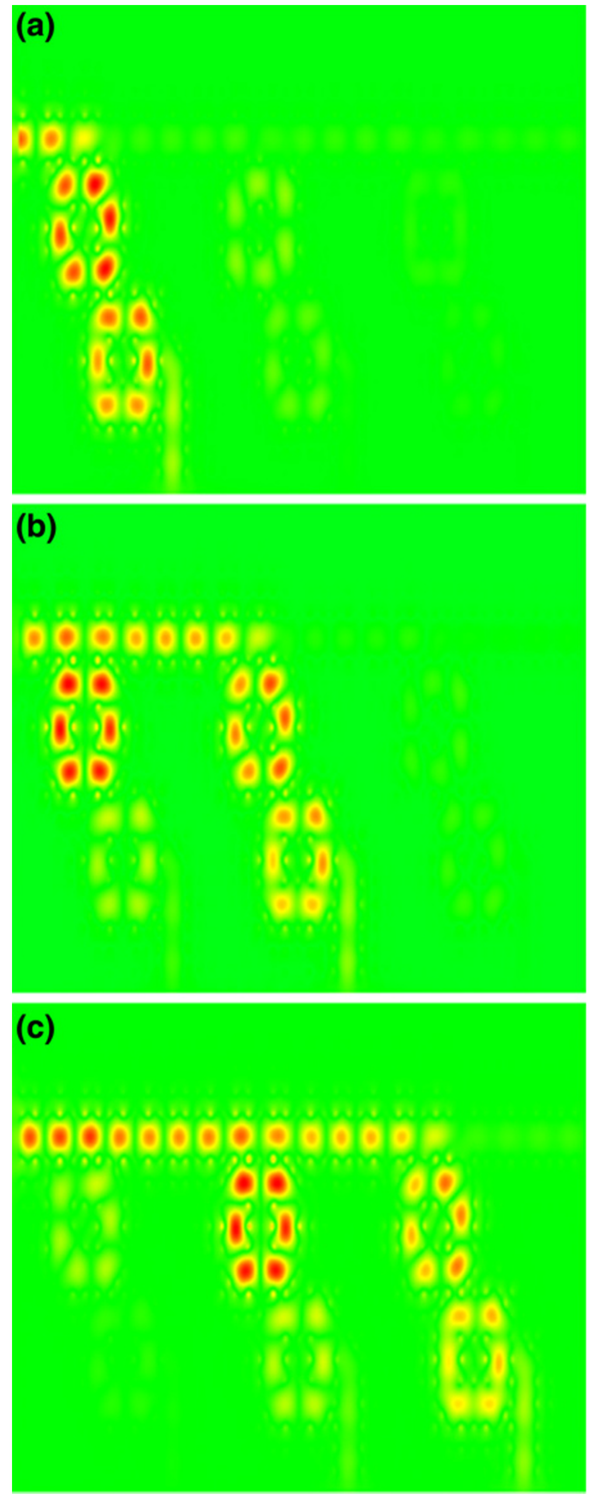

Figure 4 Light propagation inside the multichannel filter. (**a**) $\lambda_1 = 1.5889$ μm, (**b**) $\lambda_2 = 1.5786$ μm, and (**c**) $\lambda_3 = 1.5683$ μm.

Table 2 Properties of multichannel ADF based on 2-D PCRR for Gaussian input pulse with FWHM of 6 ps

Refractive index	Resonant wavelength (μm)	Output FWHM (nm)	Q-factor	Cross-talk (dB)	Time response (ps)
$n_1 = 3.79$	$\lambda_1 = 1.5889$	1.05	1,513	$XT_3 = -40$, $XT_2 = -38$	4.73
$n_2 = 3.69$	$\lambda_2 = 1.5786$	1.04	1,518	$XT_3 = -36$, $XT_1 = -35$	4.75
$n_3 = 3.59$	$\lambda_3 = 1.5683$	1.03	1,523	$XT_2 = -36$, $XT_1 = -40$	4.87

have a great impact on frequency selectivity which is an important issue in today's optical communication.

Nanoscale effects on filter's performance

In this part, the filter's operation in nanoscale regime is investigated. The filter structure is similar to the one in Figure 1, but the lattice constant is 295 nm which leads to rods' radius of 55 nm through the $r = 0.185a$ relation. In addition, the difference among refractive indices is 0.2 (i.e., indices of refraction from left to right are 3.79, 3.59, 3.39, and 3.19, correspondingly). Note that regarding $f = a/\lambda$, the reduction of lattice constant results in lower frequency, corresponding to the wavelengths in the first optical communication window.

Figure 5 and Table 3 illustrate the drop spectra and device operation for the pulse train including three Gaussian input pulses with similar FWHM of 6 ps. As can be observed in Figure 5, FWHMs of output channels are narrower, and the difference between efficiency of output channels is greater compared to Figure 3a. By comparing Tables 3 and 2, we find that for the same input FWHM, the *Q*-factor of the filter is increased significantly in nanoscale structure multichannel ADF based on 2-D PCRR. The difference between FWHM of output channels reaches 0.01 nm, while the average cross-talk is −40 dB. On the other hand, in spite of having a greater *Q*-factor, the minimum wavelength spacing is 12 nm; the average time response of the filter is longer by amount of 0.28 ps (i.e., time response ≈ 5.06 ps). Furthermore, the output channels (0.868, 0.856, and 0.844 μm) shift from the third telecommunication window to the first one with time responses of 5.23, 5.03, and 4.91 ps, respectively.

Table 3 Properties of multichannel ADF based on 2-D PCRR for Gaussian input pulse of FWHM=6 ps

Refractive index	Resonant wavelength (μm)	Output FWHM (nm)	Q-factor	Cross-talk (dB)	Time response (ps)
$n_1 = 3.79$	$\lambda_1 = 0.868$	0.31	2,818	$XT_3 = -45$, $XT_2 = -44$	5.23
$n_2 = 3.59$	$\lambda_2 = 0.856$	0.31	2,779	$XT_3 = -38$, $XT_1 = -35$	5.03
$n_3 = 3.39$	$\lambda_3 = 0.844$	0.3	2,813	$XT_2 = -41$, $XT_1 = -39$	4.91

Conclusions

In this report, multichannels ADF based on 2-D PCRR was proposed. Since add and drop operations were performed by coupling between two W1 waveguides, the heterostructure technique was employed. The wavelength spacing of 10.3 nm and average cross-talk of −37.5 dB are some features of the proposed filter. Then, the nanoscale effects on the filter's performance including wavelength spacing, cross-talk amount, and dynamic response were considered. By applying these effects, for the minimum wavelength spacing of 12 nm, the average cross-talk was −40 dB. On the other hand, in spite of greater *Q*-factor, the average time response of the system was longer by 0.28 ps.

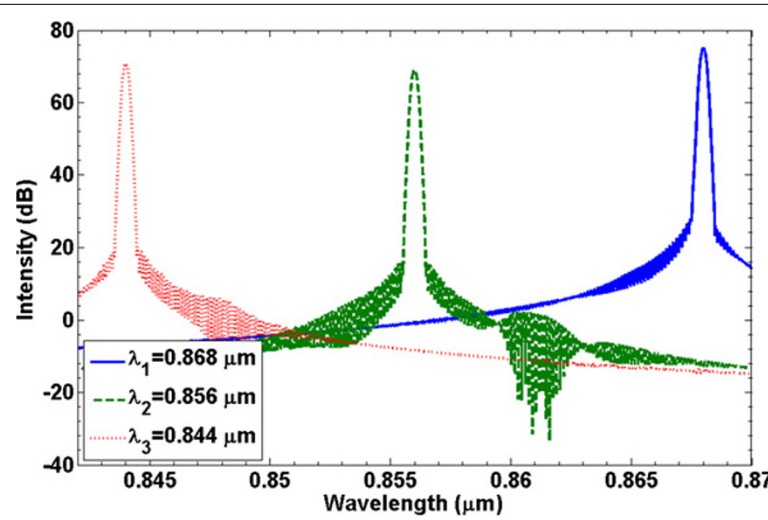

Figure 5 Drop spectra of multichannel ADF based on 2-D PCRR under nanoscale rods condition.

Competing interests
The authors declare that they have no competing interests.

Authors' contributions
Both authors read and approved the final manuscript.

Author details
[1]Department. of Electrical Engineering, Science and Research Branch, Islamic Azad University, Tehran 14778, Iran. [2]Department of Electrical and Computer Engineering, Tarbiat Modares University, Tehran 14115-194, Iran.

Received: 28 April 2012 Accepted: 17 June 2012
Published: 12 July 2012

References
1. Khitrova, G, Gibbs, HM, Jahnke, F, Kira, M, Koch, S: **Nonlinear optics of normal-mode-coupling semiconductor microcavities.** *Rev Mod Phys* 1999, **71:**1591–1639.
2. Noda, S, Chutinan, A, Imada, M: **Trapping and emission of photons by a single defect in a photonic bandgap structure.** *Nature* 2000, **407:**608–610.
3. Song, BS, Noda, S, Asano, T: **Photonic devices based on in-plane hetero photonic crystals.** *Science* 2003, **300:**1537.
4. Painter, O, Lee, RK, Scherer, A, Yariv, A, O'brien, JD, Dapkus, PD, Kim, I: **wo-Dimensional Photonic Band-Gap Defect Mode Laser.** *Science* 1999, **284:**1819–1821.
5. Noda, S, Tomoda, K, Yamamoto, N, Chutinan, A: **Full three-dimensional photonic bandgap crystals at near-infrared wavelengths.** *Science* 2000, **289:**604–606
6. Spillane, SM, Kippenberg, TJ, Vahala, KJ: **Ultralow-threshold Raman laser using a spherical dielectric microcavity.** *Nature* 2002, **415:**621–623.
7. Michler, P, Kiraz, A, Becher, C, Schoenfeld, WV, Petroff, PM, Zhang, L, Hu, E, Imamoglu, A: **A quantum dot single-photon turnstile device.** *Science* 2000, **290:**2282–2285.
8. Chiu, WY, Huang, TW, Wu, YH, Chan, YJ, Hou, CH, Chien, HT, Chen, CC: **A photonic crystal ring resonator formed by SOI nano-rods.** *Opt Express* 2007, **15:**15500–15506.
9. Qiang, Z, Zhou, W, Soref, RA: **Optical add-drop filters based on photonic crystal ring resonators.** *Opt Express* 2007, **15:**1823–1831.
10. Joannopoulos, JD, Johnson, SG, Winn, JN, Meade, RD: Photonic Crystals Molding the Flow of Light, 2nd edn. Princeton University Press, New Jersey (2008)
11. R. B. N. Inc., Characteristics of CWDM: Roots, current status, and future opportunities. Redferm Broadband Networks Inc: (2002). http://www.broadcastpapers.com/whitepapers/Characteristics-Of-CWDM-.cfm?objid = 32&pid = 340
12. Shinya, A, Mitsugi, S, Kuramochi, E, Notomi, M: **Ultrasmall multi-port channel drop filter in two-dimensional photonic crystal on silicon-on-insulator substrate.** *Opt Express* 2006, **14:**12394–12400.
13. Takano, H, Song, BS, Asano, T, Noda, S: **Highly efficient multi-channel drop filter in a two-dimensional hetero photonic crystal.** *Opt Express* 2006, **14:**3491–3496.
14. Kim S, Park I, Lim H, Kee CS: **Heterostructure wavelength division demultiplexers using photonic crystal ring resonators.** *Opt Express* 2004, **12:**5518–5525.
15. Djavid M, Monifi F, Ghaffari A, Abrishamian MS: **Highly efficient photonic crystal-based multichannel drop filters of three-port system with reflection feedback.** *Opt Commun* 2008, **281:**4028–4032.

doi:10.1186/2251-7235-6-12
Cite this article as: Pezeshki and Ahmadi: **Nanoscale effects on multichannel add/drop filter based on 2-D photonic crystal ring-resonator heterostructure.** *Journal of Theoretical and Applied Physics* 2012 **6**:12.